Short-Term Evolution of the Evening Prereversal Enhancement as Observed by ICON

Aaron Kirchman*, David Hysell
Department of Earth & Atmospheric Sciences, Cornell University, Ithaca, NY
*ajk335@cornell.edu

Summary

- The short-term evolution of the evening prereversal enhancement (PRE) of eastward electric fields, and the associated vertical drifts, is studied by comparing measurements from sequential ICON satellite orbits.
- A Gaussian curve superimposed on a linear tend parameterizes the PRE, quantifying its strength, timing, and duration.
- Changes to parameterizations indicate that the strength of the PRE can change significantly in 97 minutes and across 24 degrees longitude, the PRE structure can shift east/west relative to the terminator, and its duration can increase or decrease significantly.

Background & Motivation

The PRE is regularly observed in radar, ionosonde, and satellite observations. It has been closely related to the occurrence of F-region irregularities associated with Equatorial Spread F (ESF) [1]. **A persistence-based forecast of the PRE may improve forecasts of ESF on a night-to-night basis.**

Correlations of sequential ICON orbits suggest persistence of the PRE [4] (Figure 1). This validates the assumption used for simulating F-region irregularities using ICON drift measurements [3]. In contrast, **recent studies using ionosondes suggested rapid evolution of the PRE** [5].

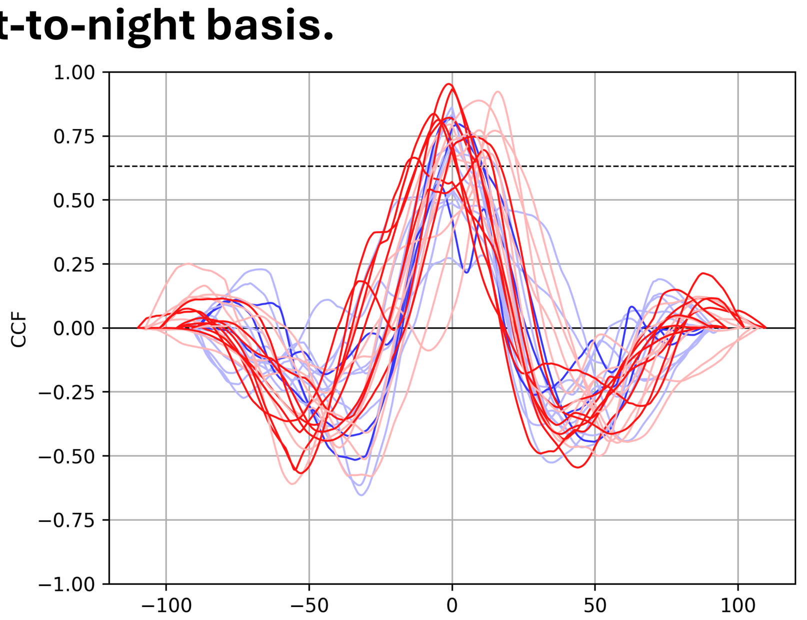

Figure 1: Cross-correlation functions for ICON vertical drifts during August (red) and October (blue) 2022. Bright (pastel) colors indicate irregularities were (were not) observed.

Using the Scherliess & Fejer 1999 empirical drifts model [6], **climatology also suggests that the PRE is a predominantly static structure**, outside of the American sector (Figure 2). Minimal changes in drifts are seen across longitudinal segments comparable to sequential ICON orbits.

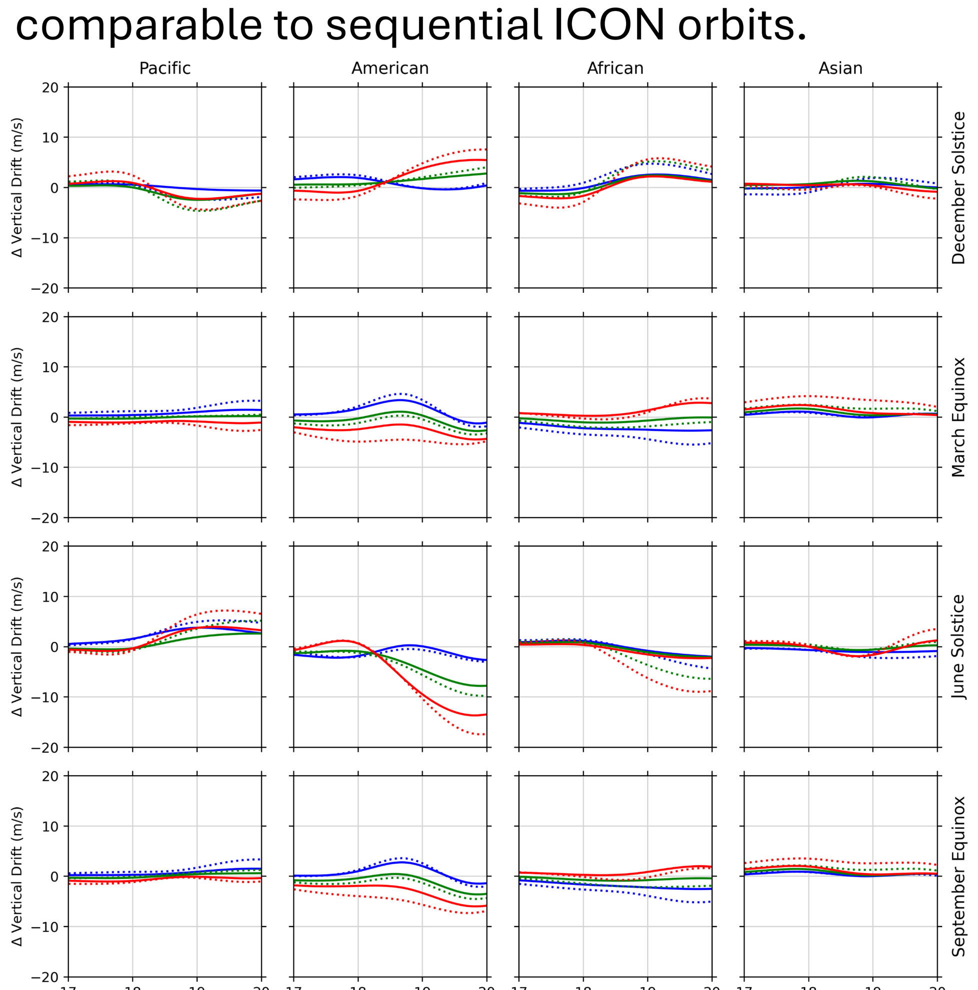

Figure 2: Climatology differences in the vertical drift velocity. Blue, green, and red curves represent low (70), medium (120), and high (170) solar flux values. Solid (dotted) curves indicate 24° (48°) longitude separation.

Methods

Vertical drift velocities are taken from the IVM-A instrument aboard ICON from November 2021 through October 2022. Drifts are averaged in 6 min. SLT bins, neglecting bins with large standard deviations (irregularities). The linear trend before and after the PRE is removed, and a Gaussian curve is used to parameterize the PRE peak (Figure 3).

Pairs of orbits are selected to compare the PRE across multiples of 97 minutes and 24 degrees longitude. Criteria for orbital pairs are as follows (Figure 4):

I. Both orbits cross the magnetic equator between 17-20 SLT.
II. Both orbits have continuous, high-quality data, with no irregularities for at least 75% of samples during 16-21 SLT.
III. Difference in magnetic equator crossing times cannot exceed 10 min.
IV. Difference in magnetic latitude is always less than 2.5 degrees during 16-21 SLT.

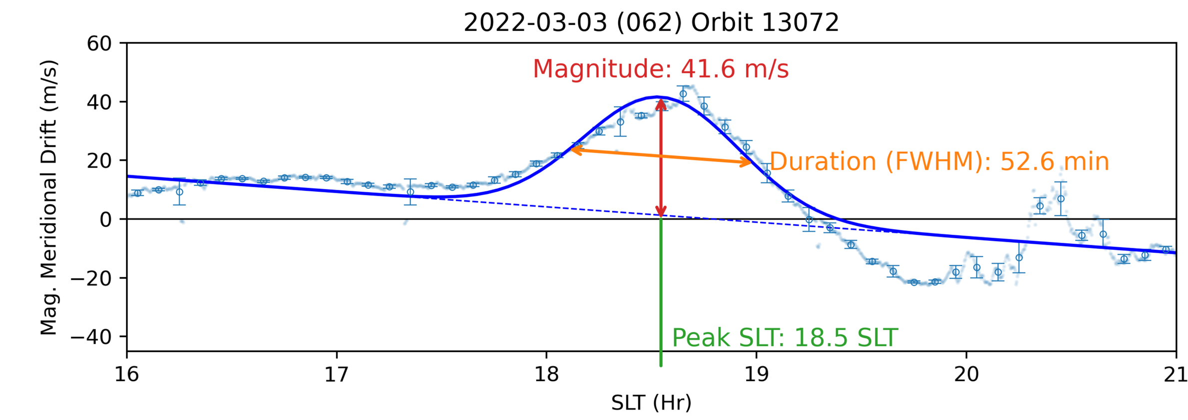

Figure 3: Example of PRE parameterization. Error bars represent 6 min. averaged IVM-A samples, the dashed line is the linear trend, and the solid curve is the full parameterization.

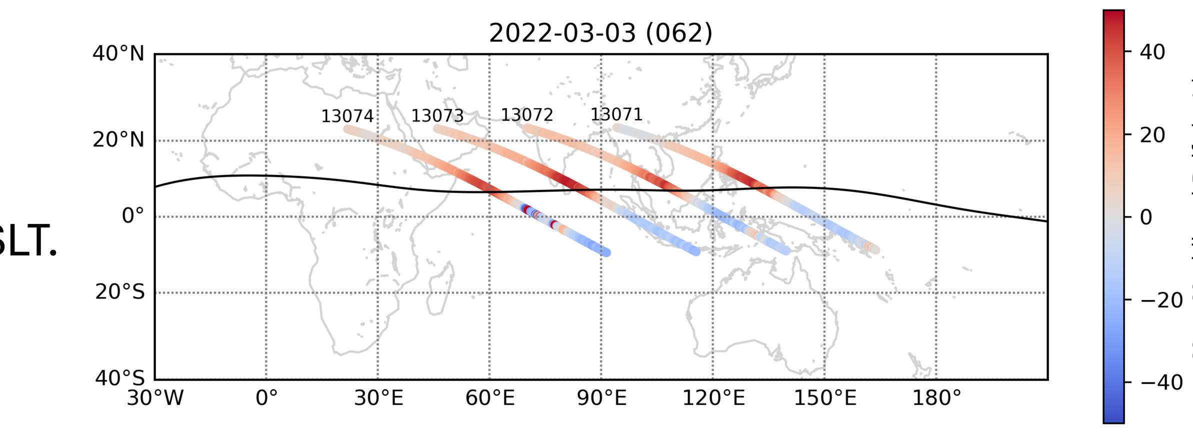

Figure 4: Vertical drifts mapped for 4 consecutive orbits satisfying conditions I-IV. Orbit numbers are labeled at 16:00 SLT.

483 individual orbits are found to satisfy conditions I and II. All of these are parameterized to determine an expected average PRE. **This produces a moderate PRE with ~20 m/s, peaking at 18:36 SLT, and lasting nearly 1.5 hours** (Figure 5). This agrees with previous ICON PRE climatology studies [2]

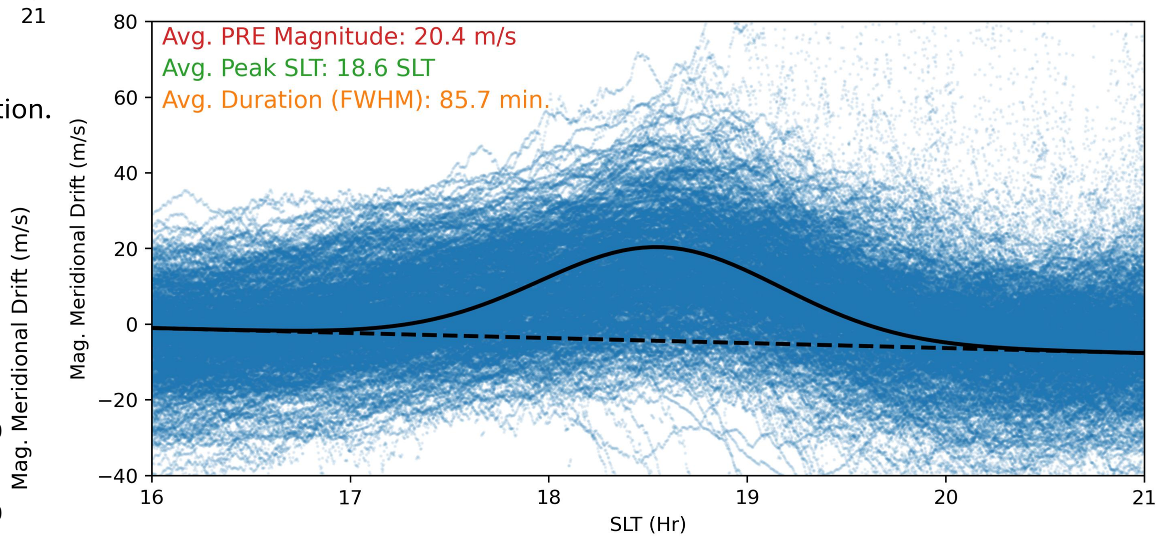

Figure 5: IVM-A measured vertical drifts from 483 individual orbits satisfying conditions I and II (blue), and the average parameterization (black).

Results

The evolution of the PRE is analyzed by comparing pairs of orbits. Similarities and differences can be seen qualitatively by plotting the two orbits on top of one another (Figure 6). Distributions of parameter differences provide statistical understanding (Figure 7). **A strongly persistent PRE should have parameter difference distributions centered on zero, with minimal standard deviation.**

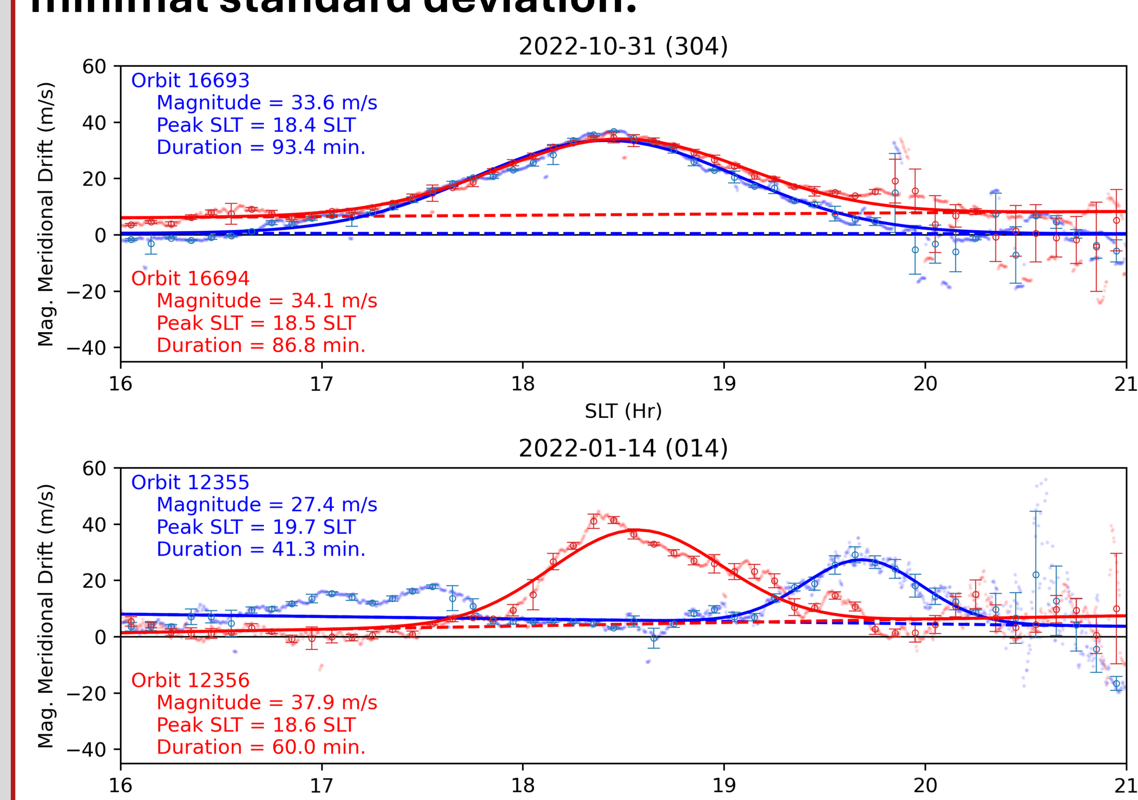

Figure 6: Examples of strong (top) and weak (bottom) persistence of the PRE. Blue (red) error bars, curves, and labels represent the first (second) orbit in the pair.

Distributions of parameter changes are primarily centered on zero but exhibit significant standard deviations. One- and two-orbit separation results are considered.

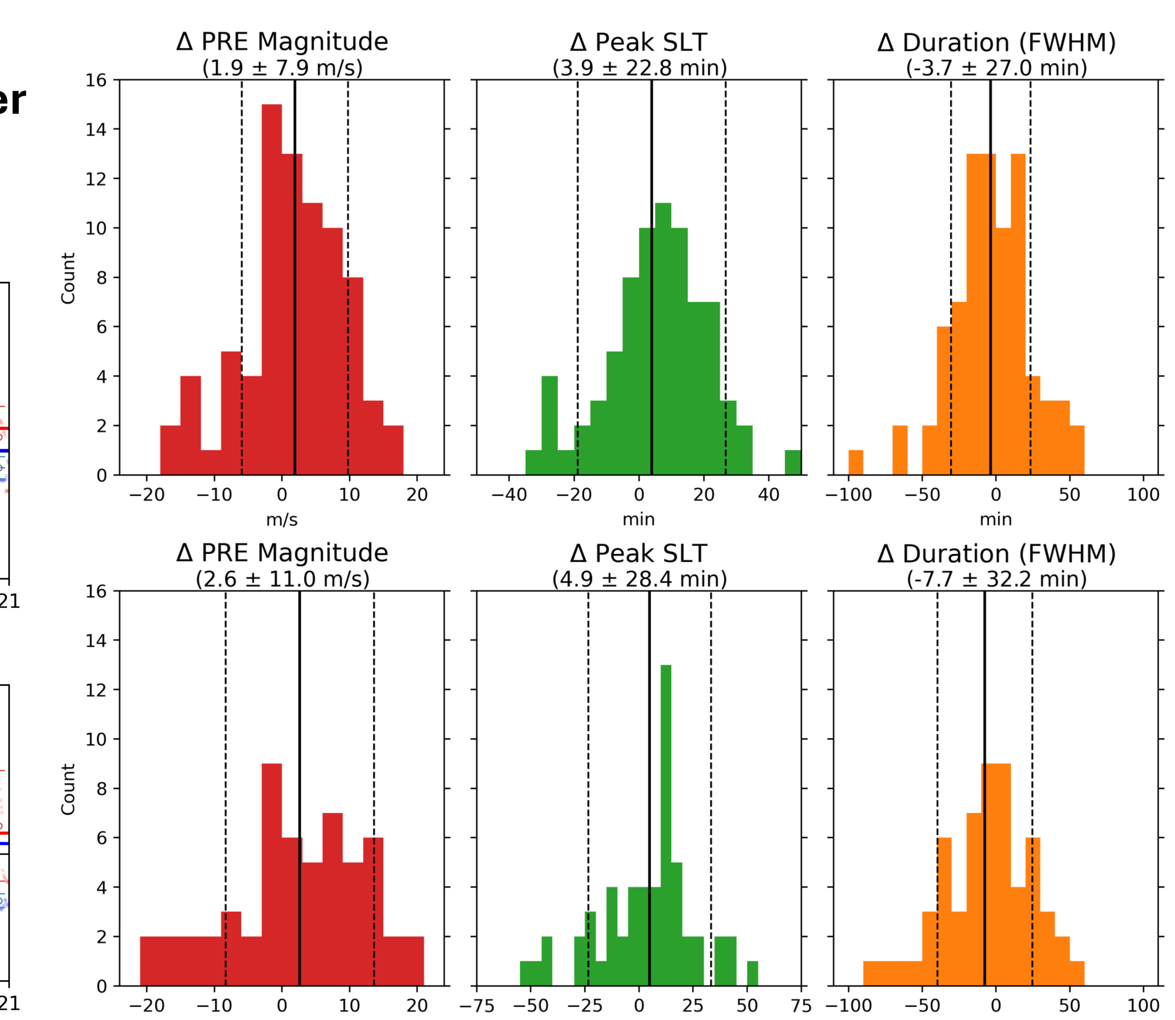

Figure 7: Distributions of PRE parameter differences with one-orbit separation (top) and two-orbit separation (bottom).

Figure 8 shows that **parameter differences exhibit no longitudinal dependency**, however, all orbital pairs investigated are in the Asian or African sector.

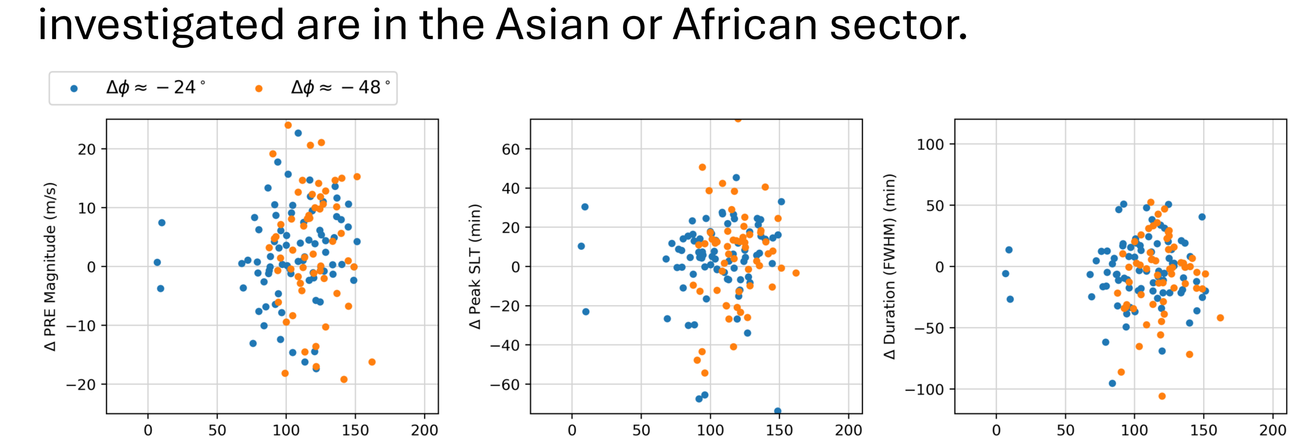

Figure 8: Longitudinal dependence of parameter differences across one-orbit separation (blue) and two-orbit separation (orange).

Figure 9 also shows **no discernible seasonal dependence for parameter differences.** More data during and after June solstice would be valuable to verify this conclusion.

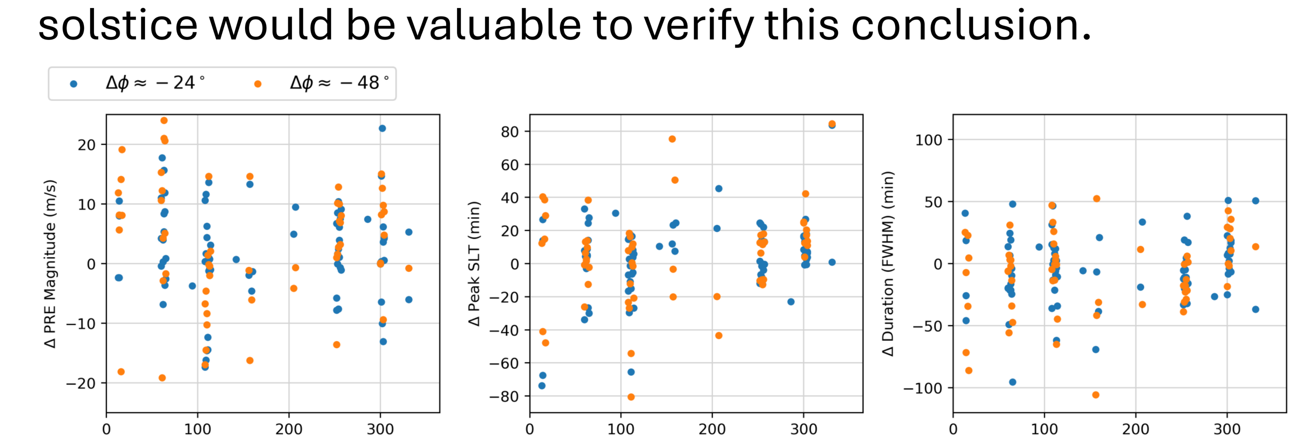

Figure 9: Seasonal dependence of parameter differences across one-orbit separation (blue) and two-orbit separation (orange).

Conclusions

- ICON observes the **PRE to be a relatively dynamic structure**, with large changes to magnitude, timing, and duration common.
- **PRE persistence is worse over longer time periods** and/or longitudinal separations.
- **Persistence-based forecasting of the PRE has limited value** because of its rapid evolution (Figure 10).

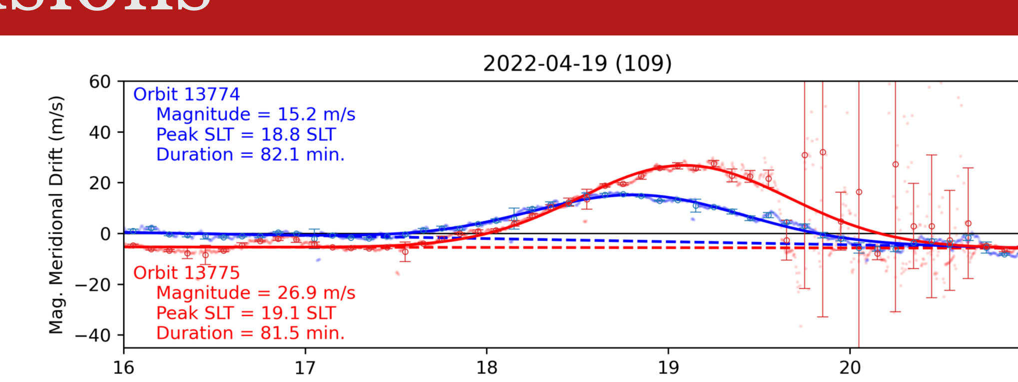

Figure 10: Example pair of orbits in which persistence-based forecasting would fail. The first orbit exhibits a weak PRE, while the second orbit exhibits a strong PRE. Large irregularities have developed by the second orbit.

References

[1] Fejer, B. G., Scherliess, L., & de Paula, E. R. (1999). Effects of the vertical plasma drift velocity on the generation and evolution of equatorial spread F. *Journal of Geophysical Research: Space Physics*, *104*(A9), 19859–19869.
[2] Harding, B. J., Serrano, M. C., Gasque, L. C., Joanne Wu, Y.-J., Maute, A., & Immel, T. J. (2025). Wind-Driven Variability in the Prereversal Enhancement of the Equatorial Vertical Plasma Drift: Climatologies Observed by ICON. *Journal of Geophysical Research: Space Physics*, *130*(1), e2024JA033279.
[3] Hysell, D. L., Kirchman, A., Harding, B. J., Heelis, R. A., England, S. L., Frey, H. U., & Mende, S. B. (2024). Using ICON Satellite Data to Forecast Equatorial Ionospheric Instability Throughout 2022. *Space Weather*, *22*(3), e2023SW003817.
[4] Kirchman, A., Hysell, D., & Fang, T.-W. (2025). Regional simulations of equatorial spread F driven with, and an analysis of, WAM-IPE electric fields. *Frontiers in Physics*, *12*.
[5] Patra, A. K., Ajith, K. K., & Perwitasari, S. (2025). On the Short-Range Longitudinal Variation of Pre-Reversal Enhancement of Vertical Plasma Drift and Associated Implications. *Journal of Geophysical Research: Space Physics*, *130*(3), e2024JA033124.
[6] Scherliess, L., & Fejer, B. G. (1999). Radar and satellite global equatorial F region vertical drift model. *Journal of Geophysical Research: Space Physics*, *104*(A4), 6829–6842.